Dynamics of the SCR-DeNO$_x$ Reaction by the Transient-Response Method

Luca Lietti, Isabella Nova, Stefano Camurri, Enrico Tronconi, and Pio Forzatti
Dipt. di Chimica Industriale e Ingegneria Chimica "G. Natta" Politecnico di Milano, P.zza L. Da Vinci 32, 20133 Milano, Italy

The unsteady-state kinetics of NH_3 adsorption–desorption and of selective catalytic reduction (SCR) of NO with NH_3 were studied over model V_2O_5/TiO_2 and $V_2O_5-WO_3/TiO_2$ catalysts by transient response techniques. Over both catalysts the dynamic experiments could be successfully described by a kinetic model assuming (1) negligible NO adsorption on the catalyst surface; (2) nonactivated NH_3 adsorption; (3) a Temkin-type NH_3 coverage dependence of the desorption energy; (4) a nonlinear dependence of the SCR reaction rate on the NH_3 surface coverage. Thus, the results are supportive of an Eley-Rideal mechanism for the SCR reaction and of a significant heterogeneity for adsorption–desorption process and surface reaction of the catalyst surface. The binary and ternary catalysts exhibit similar acid properties, but different activity in the SCR reaction, possibly related to the superior redox properties of the WO_3-containing sample. Over both samples the estimates of the activity energies for NH_3 desorption at zero coverage and for the surface reaction of NO with NH_3 are similar and in the 23–26 and 14–16 kcal/mol ranges, respectively.

Introduction

Among the various methods available for removing NO_x from stationary sources, the selective catalytic reduction (SCR) technique is the best developed and used worldwide due to its efficiency and selectivity (Bosch and Janssen, 1988; Forzatti and Lietti, 1996). The SCR process is based on the reaction between NO and NH_3 to produce water and nitrogen according to the reaction:

$$4NO + 4NH_3 + O_2 \rightarrow 4N_2 + 6H_2O.$$

Commercial SCR catalysts are made of a high-surface-area TiO_2 carrier (in the anatase form) that supports the active components of tungsten (or molybdenum) trioxide and vanadium pentoxide. Vanadia is responsible for the activity of the catalyst in the reduction of NO_x, but also for the undesired oxidation of SO_2 to SO_3; accordingly the V_2O_5 content is generally modest (0.3–1.5% w/w). WO_3 is employed in larger amounts ($\approx$ 10% w/w); it acts as a promoter by enlarging the temperature window of the SCR reaction (Chen and Yang, 1992; Lietti et al., 1996) and imparts superior thermal stability and better mechanical properties to the catalysts. Commercial catalysts are used in the form of honeycomb monoliths and plates since they offer low-pressure drops, high geometric surface areas, high attrition resistance, and low tendency to fly ash and particulate plugging.

Operation of industrial SCR monolith reactors often involves transient conditions associated with the start-up and shutdown of the plant, as well as with load variations. The SCR technology has also been proposed for NO_x abatement in systems characterized by fast load changes, such as diesel engines and heavy trucks (Andersson et al., 1994). Specific unsteady-state SCR processes (e.g., reverse-flow processes) are gaining wide interest nowadays for gas purification (Noskov et al., 1996). The understanding of the dynamics of the DeNO$_x$ reaction is of importance both in the development of unsteady processes and in the design of predictive control systems able to secure low levels of polluting emissions during both steady and transient operation.

Correspondence concerning this article should be addressed to P. Forzatti.

Although a number of studies have been devoted to mechanical and steady-state kinetics of the SCR process (Dumesic et al., 1993; Tufano and Turco, 1993; Odenbrand et al., 1994; Topsøe et al., 1995b), the precise sequence of steps involved in the reaction is still far from being completely understood. Studies on the dynamics of the reaction, on the other hand, are scarce in the literature (Andersson et al., 1994; Noskov et al., 1996; Orsenigo et al., 1996; Tronconi et al., 1996). In view of this situation, a study of the $DeNO_x$ reaction under nonstationary conditions has been undertaken in our laboratories in order to gain additional insight into the adsorption–desorption characteristics of the reactants NH_3 and NO, and into the mechanics and the dynamic behavior of the reaction. The transient-response method described by Kobayashi and Kobayashi (1974) has been applied for this purpose. In a typical transient-response experiment, perturbations are imposed to the reacting system (e.g., step changes in the inlet reactant concentration) and the transient response is analyzed. The characteristics of the response reflect the nature of the sequence of steps underlying the kinetics of the reaction: therefore these methods are able to provide mechanistic evidence that cannot be collected under steady-state conditions, since in this case all the elementary steps of the reaction are progressing at the same rate and hence the precise kinetic structure of the reaction can hardly be identified.

To obtain quantitative kinetic indications, then, the results of the transient-response experiments have been analyzed according to a simple dynamic model of the reacting system, and the rate parameters for adsorption–desorption of the reactants and for their surface reaction have been estimated, being relevant to unsteady-state modeling of the monolithic SCR reactors.

Experimental Studies

Catalysts

Binary V_2O_5/TiO_2 ($V_2O_5 = 1.47\%$ w/w) and ternary $V_2O_5–WO_3/TiO_2$ ($V_2O_5 = 1.47\%$ w/w and $WO_3 = 9\%$ w/w) model catalysts were used in this study. The binary V_2O_5/TiO_2 sample was prepared by dry impregnation of TiO_2 anatase calcined at 823 K for 2 h with a water solution of ammonium metavanadate and oxalic acid, followed by drying and calcination at 823 K (Lietti and Forzatti, 1994). The $V_2O_5–WO_3/TiO_2$ catalyst was prepared by first impregnation the TiO_2 support with a hot-water solution of ammonium paratungstate and citric acid, followed by drying and calcination at 823 K. Vanadium was then introduced by dry impregnation of the calcined WO_3/TiO_2 samples with a hot-water solution of ammonium metavanadate and oxalic acid, followed by drying and calcination at 823 K (Alemany et al., 1995).

The XRD analysis showed that the catalysts are monophasic and constituted by TiO_2 in the polymorphic form of anatase. The specific surface area (S_a) of the V_2O_5/TiO_2 sample is 46 m^2/g, whereas that of the ternary $V_2O_5–WO_3/TiO_2$ catalyst is 80 m^2/g. The V, W, and (W+V) surface coverage (θ_V, θ_W, and θ_{V+W}, respectively), calculated as reported by Vermaire and van Berge (1989) and by Bond and Tahir (1991), are $\theta_v = 0.21$ for the V_2O_5/TiO_2 sample (and hence $\theta_{Ti} = 0.79$) and $\theta_v = 0.12$, $\theta_w = 0.67$ for the $V_2O_5–WO_3/TiO_2$ catalyst ($\theta_{v+w} = 0.79$, $\theta_{Ti} = 0.21$).

Apparatus for transient adsorption–desorption of the reactants and reactivity experiments

The transient kinetic runs of NH_3 and NO adsorption–desorption and of $NO+NH_3$ reaction were performed in a flow-microreactor system. The feed gases (0.5% NH_3 in He, 0.5% NO in He, 2% O_2 in He, and 0.5% Ar (inert tracer) in He), whose flow rates were measured and controlled by mass-flow controllers (Brooks 5850 TR), were mixed in a single stream before entering the reactor. A four-port valve was used to perform the abrupt switches between NH_3/He and NO/He. Care was taken in minimizing all possible dead volumes in the lines before and after the reactor and in eliminating pressure and flow changes upon switching of the reactants.

The reactor consisted in a quartz tube (9-mm OD, 6-mm ID) with a tapered exit (2-mm ID) directly connected to a mass spectrometer (UTI 100C) by a leaking system constituted of two calibrated orifices (30 μm) with differential pumping in between. This system allowed fast transfer of the gases from the reactor to the quadrupole mass analyzer (traveling time lower than 2 s). The reactor was inserted into an electric furnace driven by a proportional-integral-derivative controller, and the catalyst temperature was measured and controlled by means of a *K*-type thermocouple directly immersed in the catalyst bed.

One hundred and sixty milligrams of catalyst with small particle diameter (60–100 mesh) were used in each run in order to minimize diffusional intrusions. The absence of both interphase and intraparticle concentration gradients was verified according to diagnostic criteria (Mears, 1971; Froment and Bishoff, 1979; Tronconi and Forzatti, 1986).

The following mass-to-charge (m/e) ratios were used to monitor the concentration of products and reactants: 17 (NH_3), 18 (H_2O), 28 (N_2), 30 (NO), 32 (O_2), 44 (N_2O), and 46 (NO_2). The mass-spectrometer data were quantitatively analyzed using the fragmentation patterns and the response factors determined experimentally from calibration gases. The interference of H_2O on m/e 17 and of N_2O on m/e 28 and 30 was taken into account in determining the products composition.

Nitrogen balances, performed on the gases exiting from the reactor under steady-state conditions, always closed within $\pm 5\%$.

Transient adsorption–desorption study of the reactants

The kinetics of the transient adsorption–desorption of the reactants (NH_3 and NO) were investigated by imposing stepwise perturbations in the NH_3 and NO reactor inlet concentration. In a typical experiment, the catalyst was loaded in the reactor and oxidized at 773 K for 1 h in He+20% O_2. Then a stream of He+1% v/v O_2 (120 cm^3/min STP) was fed to the reactor and the catalyst temperature was set at the desired value. After stabilization of the MS signals, a rectangular step feed of ammonia or NO (0 → 700 ppm) was admitted to the reactor at constant temperature, keeping the overall carrier gas flow rate constant at 120 cm^3/min STP. Then the NH_3 (or NO) concentration was stepwise decreased (700

→ 0 ppm), and after ≈ 10 min the catalyst was heated up to 773 K under temperature programming at 15 K/min in order to completely desorb the reactants still adsorbed over the catalyst surface [temperature-programmed desorption, (TPD)].

Transient DeNO$_x$ reaction study

The dynamics of the SCR reaction were investigated by imposing stepwise perturbations (0 → 700 ppm and 700 → 0 ppm) in the NH_3 (or NO) reactor inlet concentration while keeping constant the concentrations of the other reactants. Accordingly, when the NH_3 (or NO) inlet concentration was varied, a stream consisting of He + 1% O_2 + 700 ppm NO (or 700 ppm NH_3) was steadily flowing in the reactor. The total flow rate was always set at 120 cm^3/min STP.

Blank experiments

A series of blank experiments were performed to examine the response of the system upon step changes in the inlet NH_3 and NO concentration in the absence of a catalyst. This was accomplished by performing both transient NH_3 and NO adsorption–desorption experiments and transient DeNO$_x$ reaction experiments in a reactor where the catalyst had been replaced by quartz granules having the same size (60–100 mesh). These blank experiments were performed at the same temperatures used for the transient adsorption–desorption and reactivity studies.

During blank experiments, the formation of reaction products was never observed, thus indicating that the influence of homogeneous uncatalyzed gas-phase reactions is negligible. A comparison between the ideal inlet concentration and the measured reactor outlet concentration is reported in Figure 1, for a NH_3 switch experiment taken as an example. The figure clearly shows that both the dead time and the broadening of the response due to axial dispersion in the system is limited: accordingly an ideal plug-flow reactor model has been applied to the analysis of the transient-response experiments.

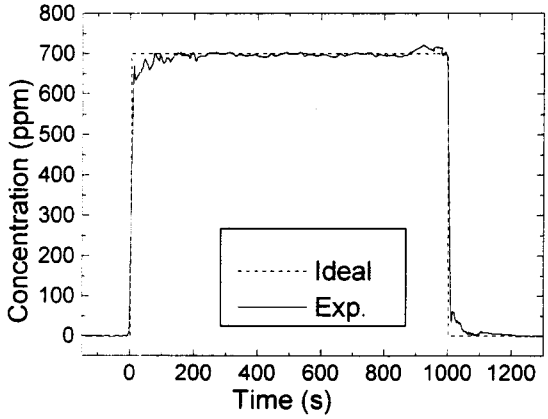

Figure 1. Typical blank NH_3 step-feed experiment performed in He+1% O_2 at T = 623 K.

The dotted line represents the ideal NH_3 inlet concentration.

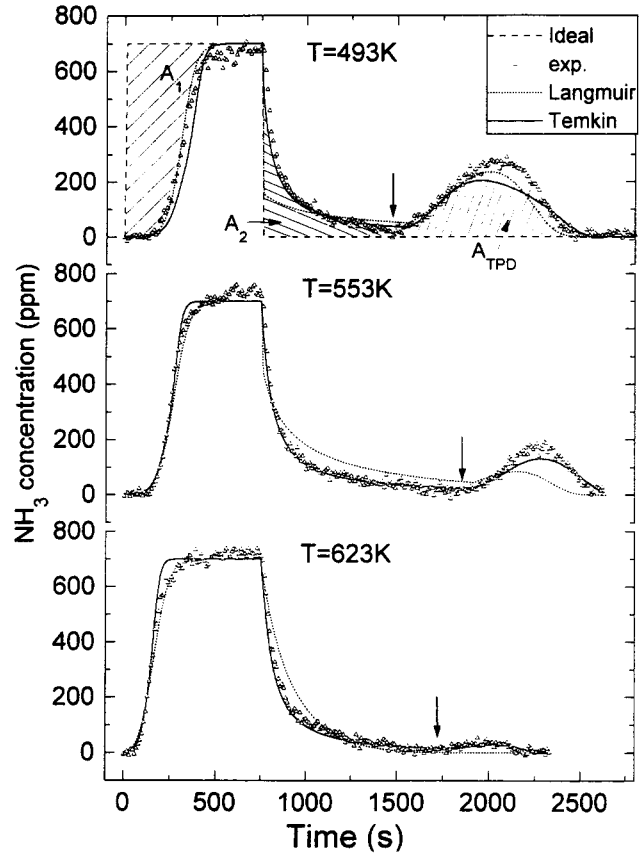

Figure 2. Dynamic adsorption–desorption of NH_3 on a model V_2O_5/TiO_2 catalyst following a NH_3 step addition (at t = 0 s), shut-off (at t = 750 s) and thermal desorption (TPD).

Experimental data (symbols) and model fit. Dotted lines: Langmuir coverage dependence of the desorption energy; solid lines: Temkin coverage dependence. The ideal inlet NH_3 concentration is also reported (dashed lines). The arrows indicate the start of the TPD runs.

Results

Transient kinetics of the adsorption–desorption of NH_3 and NO

NH_3 Adsorption–Desorption in He + O_2. A typical result obtained in the case of a rectangular step feed of ammonia performed in flowing He + 1% v/v O_2 over the binary V_2O_5/TiO_2 model catalyst at different temperatures (493, 553, and 623 K) is presented in Figure 2, along with the ideal ammonia inlet concentration (reported only for T = 493 K, dashed lines). The results of the TPD experiment obtained upon heating the catalyst at the end of the ammonia rectangular pulse are also shown (righthand side of the figure).

In the case of the experiments performed at 493 K, Figure 2 shows that upon the NH_3 step addition (at t = 0 s), the ammonia outlet concentration slowly increased with time, approaching the ammonia inlet concentration (700 ppm) only after ≈ 500 s. The area included between the ammonia inlet and outlet concentration traces (shaded area A_1 of the figure) is proportional to the amount of NH_3 adsorbed over the catalyst surface. A value of 3.62×10^{-3} mol$_{NH_3}$/m^2 was estimated in this case. A similar behavior is apparent upon am-

monia shutoff ($t = 750$ s): the outlet NH_3 concentration slowly decreases with time due to the desorption of previously adsorbed ammonia. Complete desorption of NH_3 was achieved upon subsequent heating of the catalyst (TPD experiment), as also indicated by the area underlined by the TPD trace ($A_{TPD} + A_2 = A_1$).

On increasing the catalyst temperature the variations in the ammonia outlet concentration during the adsorption step are faster and the amount of ammonia adsorbed on the catalyst surface is reduced, in line with the increased rates of the adsorption–desorption processes and with the exothermicity of the NH_3 adsorption process. Accordingly, the area of the TPD desorption trace is also significantly reduced, being almost negligible when the NH_3 adsorption/desorption is carried out at 623 K.

NH_3 adsorption experiments were also carried out at higher temperatures (> 623 K), but in this case the formation of N_2, N_2O, and H_2O has been observed, indicative of the occurrence of the ammonia oxidation reaction. For this reason, these experiments have not been considered for further analysis, and results will not be presented in the following.

Similar NH_3 adsorption–desorption transient experiments were performed at various temperatures over the ternary V_2O_5–WO_3/TiO_2 model catalyst. The results of the dynamic NH_3 adsorption–desorption experiments performed at 553 K over the ternary catalyst are reported in Figure 3, where they are compared with those obtained in the case of the binary V_2O_5/TiO_2 sample. As shown in Figure 3, the transient responses recorded over the two catalysts during both the NH_3 step addition and shutoff experiments and the TPD runs are very similar. It is noted, however, that in the case of the ternary catalyst the ammonia adsorption study could not be performed at temperatures exceeding 553 K due to the occurrence of the NH_3 oxidation reaction. This clearly indicates the higher reactivity of V_2O_5–WO_3/TiO_2 in the ammonia oxidation reaction.

Kinetic Analysis of the NH_3 Adsorption–Desorption Experiments. The features of the NH_3 gas-phase concentration profiles vs. time obtained under transient conditions are representative of the kinetics of the adsorption–desorption processes occurring at the catalyst surface. Accordingly, the results were analyzed by a dynamic reactor model and fitted by nonlinear regression to provide estimates of the relevant kinetic parameters. In line with the results of the blank experiments previously reported, the contributions of axial dispersion and of dead time were disregarded and an ideal isothermal plug-flow reactor model was adopted. Also, on the basis of theoretical diagnostic criteria (Mears, 1971), the influence of both intraparticle catalyst gradients and external mass-transfer limitations were estimated as negligible. Under these simplifying hypotheses, the unsteady-state NH_3 mass balances on the catalyst surface and in the gas stream were written as

$$\frac{\partial \theta_{NH_3}}{\partial t} = r_a - r_d \tag{1}$$

$$\frac{\partial C_{NH_3}}{\partial t} = -v\frac{\partial C_{NH_3}}{\partial z} + \Omega(r_d - r_a), \tag{2}$$

where the symbols are defined in the Notation section. The following rate expressions have been used for NH_3 adsorption and desorption from the catalyst surface:

$$r_a = k_a^0 \exp(-E_a/RT) C_{NH_3}(1-\theta_{NH_3}) \tag{3}$$

$$r_d = k_d^0 \exp(-E_d/RT)\theta_{NH_3}. \tag{4}$$

Equations 1–4 were solved by standard numerical procedures (Finlayson, 1980; Hindmarsh, 1983). On the basis of preliminary fits of the experimental data, it was found that the NH_3 adsorption occurs by a nonactivated process ($E_a = 0$), in line with the spontaneity of adsorption of a basic molecule, like ammonia, over the acid catalyst surface (Lietti et al., 1993; Lietti and Forzatti, 1994; Srnak et al., 1992). Different rate expressions were used for NH_3 desorption, including a simple Langmuir approach (that considers a constant value of the desorption activation energy E_d), and more complicated expressions that take into account the catalyst surface heterogeneity, in agreement with the physicochemical characterization of the catalysts (Topsøe, 1991; Ramis et al., 1992; Lietti et al., 1993). These included Temkin-type [$E_d = E_d^0(1-\alpha\theta_{NH_3})$], modified Temkin-type [$E_d = E_d^0(1-\alpha\theta_{NH_3}^{\sigma})$], and Freundlich [$E_d = E_d^0 \exp(-\alpha\theta_{NH_3})$] coverage dependence of the desorption energies, along with an empirical coverage dependence that is representative of the existence of two adsorption sites on the catalyst surface having different acid strength ["dual sites" coverage dependence, $E_d = E_d^0 + B\tanh(-\alpha\theta_{NH_3} + A)$]. Figure 2 compares the experimental data of the adsorption–desorption experiments, followed by the TPD runs with typical model fits obtained by global nonlinear regression, minimizing the squared errors between the model predictions and the actual NH_3 concentration profiles of the adsorption–desorption experiments performed at different temperatures (493, 553 and 623 K), followed by the TPD runs. The results corresponding to the Langmuir-type (dotted lines) and the Temkin-type (solid lines) coverage dependence are shown. The figure clearly shows that the Langmuir kinetics fail in describing accurately the experimental data, and particularly in the case of the NH_3 desorption process. A reasonable fit is obtained only at the

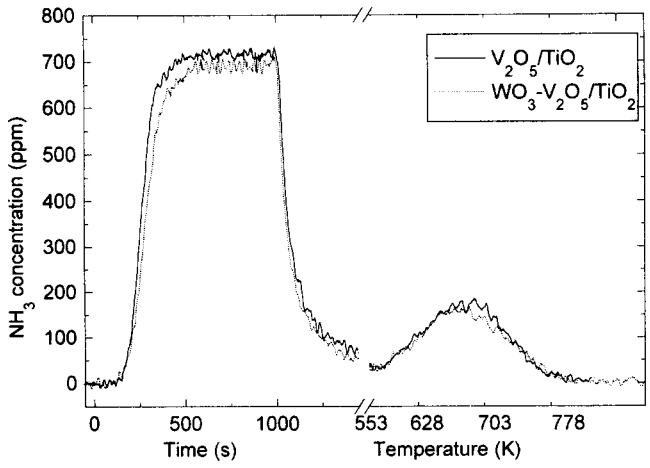

Figure 3. Dynamic NH_3 adsorption–desorption for: binary (solid line) and ternary catalyst (dotted line) at $T = 553$ K.

Table 1. Estimates of Kinetic Parameters for NH_3 Adsorption–Desorption over V_2O_5/TiO_2 and V_2O_5–WO_3/TiO_2 Catalysts*

Parameters	V_2O_5/TiO_2	95% Confidence Limits	V_2O_5–WO_3/TiO_2	95% Confidence Limits
k_a^0 (m^3/mol·s)	0.820	±0.045	0.487	±0.038
k_d^0 (1/s)	3.67×10^6	$\pm0.95\times10^6$	2.67×10^5	$\pm0.11\times10^5$
E_d^0 (kcal/mol)	25.8	±0.1	22.9	±0.2
α	0.310	±0.013	0.405	±0.023
Ω (mol/m^3)	209	±5	270	±11

*Temkin-type NH_3 coverage dependence of the desorption energy leading to the fits in Figure 2 (solid lines).

highest investigated temperatures, where ammonia is bound to the strongest adsorption sites that likely exhibit similar acid strengths.

As shown in Figure 2, a satisfactory data fit was achieved by using a nonactivated NH_3 adsorption process and a Temkin-type desorption kinetics that implies a linear decrease in the activation energy for desorption with the NH_3 surface coverage. These results are in line with the presence of distinct types of acid sites (e.g., Lewis and/or Bronsted) characterized by different acid strengths (Topsøe, 1991; Ramis et al., 1990, 1991, 1992; Lietti et al., 1993; Schneider et al., 1994). We note that no further significant improvements were obtained by using more complicated coverage dependence of the desorption energies (e.g., modified Temkin-type or the empirical "dual sites").

The estimates of the kinetic parameters leading to the fits of Figure 2 together with their confidence limits are reported in Table 1. The optimal parameter estimates yield an activation energy for NH_3 desorption at zero coverage (E_d^0) close to 25 kcal/mol. It is worth emphasizing that the model accounts quite satisfactorily for large variations in the NH_3 surface coverage (θ_{NH_3} was estimated to vary in the range 0–0.8) and/or in the catalyst temperature ($T = 493-623$ K). Particularly demanding in this respect are the TPD experiments where both the NH_3 surface coverage and the catalyst temperature vary simultaneously over a wide range.

A satisfactory fit of the data has also been obtained in the case of the ternary V_2O_5–WO_3/TiO_2 model catalyst. As reported in Table 1, the parameter estimates for NH_3 adsorption–desorption are similar to those obtained over the binary V_2O_5/TiO_2 sample. The slightly higher value of the catalyst capacity ($\Omega = 270$ vs. 209 mol_{NH_3}/m^3) seems to be primarily due to the higher specific surface area of the V_2O_5–WO_2/TiO_2 catalyst with respect to the V_2O_5/TiO_2 binary sample (80 vs. 46 m^2/g).

NO Adsorption–Desorption in He + O_2. Rectangular step feeds of NO in He + 1% O_2 were performed at different temperatures over both the binary and the ternary V_2O_5–WO_3/TiO_2 model catalysts. In all cases the outlet NO concentration curves closely resemble that of the inlet NO concentration; the results are similar to those of blank experiments performed with an inert tracer shown, for example, in Figure 1. This indicates that NO does not appreciably adsorb onto the catalyst surface, which is in line with several indications in the literature (Srnak et al., 1992; Topsøe et al., 1995b).

Transient kinetics of SCR of NO by NH_3

NH_3 Step Feed in He + O_2 + NO. Figure 4 shows typical results obtained over the ternary V_2O_5–WO_3/TiO_2 sample upon performing a positive ($C_{NH_3} = 0 \rightarrow 700$ ppm, $t = 0$ s) and a negative ($C_{NH_3} = 700 \rightarrow 0$ ppm, $t = 1{,}250$ s) step change of the NH_3 feed at 493 K in flowing He + NO 700 ppm + O_2 1% v/v. The figure reports the evolution with time of ammonia (curve *a*), nitrogen oxide (curve *b*), and nitrogen (curve *c*) concentrations.

Upon the NH_3 step feed ($t = 0$), the NO reactor outlet concentration decreased due to the occurrence of the SCR reaction. The evolution with time of the ammonia, NO and N_2 concentrations show different transient behaviors: the ammonia concentration profile exhibits a dead time (≈ 250 s) and then slowly increases with time on stream to the new steady-state value, that is reached only after 800 s. On the other hand, the NO concentration trace does not show any dead time and suddenly decreases to its new steady-state

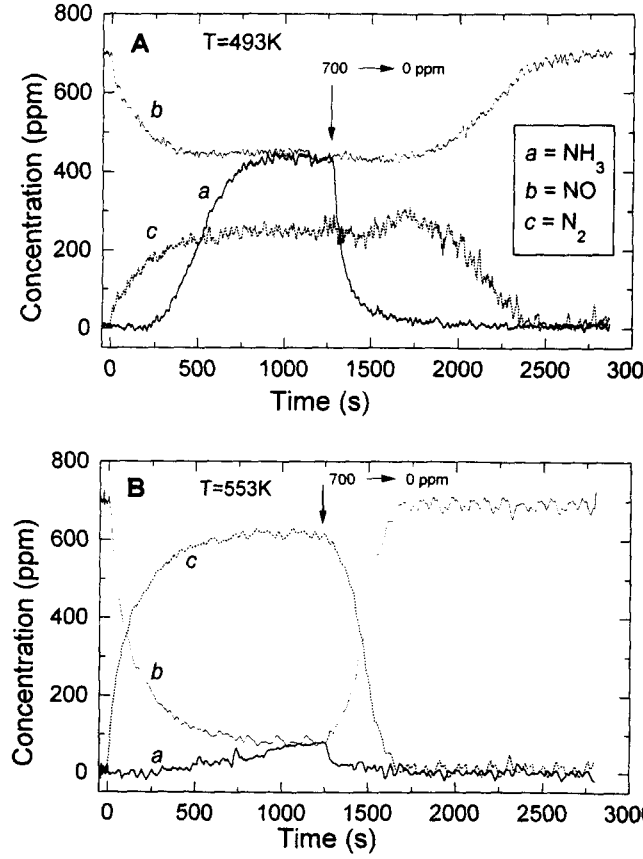

Figure 4. NH_3 step-feed ($t = 0$ s) and shutoff (arrows at $t = 1{,}250$ s) experiments in He + O_2 (1% v/v) + NO (700 ppm) over the WO_3–V_2O_5/TiO_2 catalyst: (A) $T = 493$ K; (B) $T = 553$ K.

value, reached after 300 s. The evolution with time of N_2 and of H_2O (not reported in the figure) is specular to that of NO. No formation of other species (e.g., N_2O) was observed, thus indicating the occurrence of a genuine SCR process.

A different transient behavior is observed upon the NH_3 shutoff, performed at $t = 1{,}250$ s and indicated with an arrow in Figure 4A. Indeed whereas the NH_3 concentration rapidly dropped to zero, the NO concentration signal was not apparently affected; only after several minutes it began to increase up to the inlet concentration value. Again the N_2 concentration trace is specular to that of NO; however, in this case a weak maximum is evident near 1,700 s, whose origin has not been clearly understood so far.

The observed transient responses are typical of a reaction involving a strongly adsorbed species (NH_3) and a gas phase or weakly adsorbed species (NO). Indeed, in correspondence of the ammonia step addition, adsorbed NH_3-related reactive species are formed, leading to the immediate consumption of gaseous NO. Accordingly, whereas the ammonia outlet concentration signal slowly increases with time on stream (NH_3 being involved in adsorption–desorption processes), the NO concentration rapidly decreases. On the other hand, upon the NH_3 shutoff at $t = 1{,}250$ s, ammonia adsorbed species are still available for the reaction, and accordingly NO is still converted. It is worth noting that this process lasts for several minutes, as indicated by the fact that the NO (reagent) and N_2 (product) concentration traces do not change with time on stream in spite of the fact that the NH_3 reactor inlet concentration has been zeroed. This clearly indicates that the rate of the SCR reaction does not depend on the ammonia surface concentration above a characteristic "critical" value of the NH_3 coverage. Also, it is noted that the evolution of N_2 and of H_2O, specular to that of NO, indicates that the formation of these reaction products is not desorption-limited. These points are discussed further in the following.

Similar evolution of the concentrations of ammonia, nitrogen oxide, and nitrogen with time on stream were obtained by performing the NH_3 step feed experiments at higher temperatures (553 and 623 K), as presented in Figure 4B for $T =$ 553 K. A comparison with Figure 4A shows that, on increasing the reaction temperature: (1) the steady-state concentration of NO is lowered; (2) the initial NO concentration level is rapidly restored after NH_3 is shut off (arrow at $t \approx 1{,}250$ s), the delay observed in Figure 4A being no longer apparent. The same effects were even more evident at the highest investigated temperature (623 K): the results are not reported for brevity. Such temperature effects are explained by the higher rates both of NH_3 desorption and of the surface reaction, which result in a higher conversion of NO but also in a significant depletion of the adsorbed ammonia. Under these conditions (low NH_3 surface coverage) the rate of NO consumption becomes directly dependent on the ammonia surface concentration, so that the temporal evolution of NO follows closely that of NH_3.

The same kind of experiments were repeated using the binary V_2O_5/TiO_2 sample, with qualitatively similar results. Figure 5 shows a comparison of the NH_3 and NO transient behavior obtained at 553 K upon a NH_3 step feed addition to the binary (solid lines) and the ternary (dotted lines) V_2O_5–WO_3/TiO_2 catalyst. In spite of the different steady-state levels measured over the two samples, indicating a

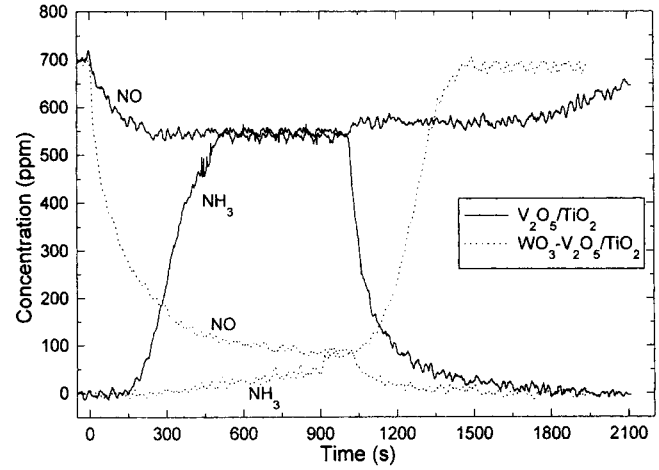

Figure 5. NH_3 step-feed and shutoff experiments in He $+O_2$ (1% v/v)+NO (700 ppm) performed over: binary V_2O_5/TiO_2 (solid lines) and ternary (dotted lines) WO_3–V_2O_5/TiO_2 catalysts at 553 K.

greater reactivity of the WO_3-containing catalyst, the transient behaviors are qualitatively similar. The higher reactivity of the ternary catalyst in the SCR reaction with respect to the corresponding V_2O_5/TiO_2 samples is well documented in the literature (Lietti et al., 1996).

NO Step Feed in He + O_2 + NH_3. Figures 6A and 6B show typical results obtained upon performing a rectangular step feed of NO at 493 and 553 K, respectively, over the ternary V_2O_5–WO_3/TiO_2 sample. The figure reports the evolution with time of ammonia (triangles) and nitrogen oxide (circles) concentrations.

Upon the NO step feed ($t = 0$ s) the NH_3 reactor outlet concentration immediately decreases due to the occurrence of the SCR reaction, and a parallel evolution of N_2 and of water (not reported in the figure) is observed. The evolution with time on stream of ammonia and NO concentrations upon the NO step feed performed at $t = 0$ s significant differs from those monitored during the corresponding NH_3 step feed experiments reported in Figures 4A and 4B. In particular the concentration products and reactants reach their steady-state values rapidly, in contrast to what was observed when the inlet NH_3 concentration was varied in a stepwise manner. These results further confirm that NO is not involved in an adsorption–desorption process on the catalyst surface, and that the SCR reaction occurs between a strongly adsorbed NH_3 species and a gas-phase or weakly adsorbed NO molecule according to an Eley–Rideal mechanism.

Similar results (not reported for the sake of brevity) were obtained over the binary V_2O_5/TiO_2 sample. However, in this case lower NO conversions were measured at the same reaction temperatures if compared to the ternary catalyst, in line with the lower reactivity of the binary sample in the SCR reaction.

Kinetic Analysis of the SCR Transient Experiments. The results of the NH_3 step feed experiments performed at different temperatures (Figures 4 and 5) have been analyzed according to a dynamic one-dimensional heterogeneous PFR model and fitted by nonlinear regression to estimate the kinetic parameters.

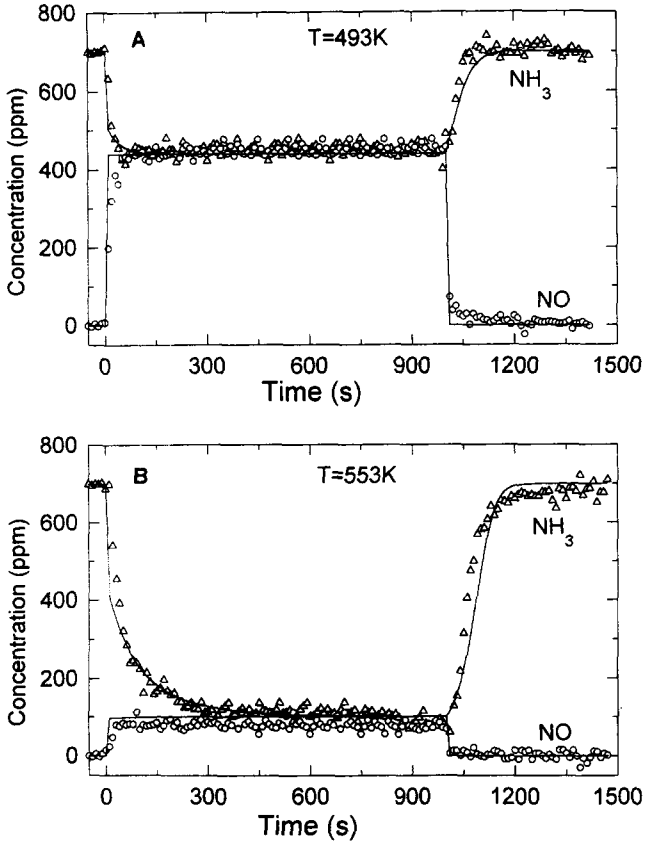

Figure 6. NO step-feed ($t = 0$ s) and shutoff ($t = 1{,}000$ s) experiments in $He + O_2$ (1% v/v) + NH_3 (700 ppm) over the WO_3–V_2O_5/TiO_2 catalyst.

Experimental data (symbols) and model predictions (solid lines) obtained with the parameters reported in Table 2; (A) T = 493 K; (B) T = 553 K.

The unsteady mass balance of NH_3 on the catalyst surface, Eq. 1, was modified to include a term accounting for NH_3 consumption by the SCR surface reaction (r_{NO}) as follows:

$$\frac{\partial \theta_{NH_3}}{\partial t} = r_a - r_d - r_{NO}. \tag{1b}$$

The following NO unsteady mass balance in the gas stream was also included:

$$\frac{\partial C_{NO}}{\partial t} = -v\frac{\partial C_{NO}}{\partial z} - \Omega r_{NO} \tag{5}$$

in addition to the unsteady mass balance of gaseous NH_3, Eq. 2.

In line with the results of the ammonia dynamic adsorption–desorption study, a nonactivated adsorption process and a Temkin-type coverage dependence of the desorption energy were considered for NH_3:

$$r_a = k_a^0 C_{NH_3}(1 - \theta_{NH_3}) \tag{3b}$$

$$r_d = k_d^0 \exp\left(-E_d^0(1 - \alpha\theta_{NH_3})/RT\right)\theta_{NH_3}. \tag{4b}$$

Different rate expressions have been tested for the SCR reaction (r_{NO}), including first-order kinetics in respect to θ_{NH_3} (*model a*, Eq. 6a) and "modified" θ kinetics (*model b*, Eq. 6b):

$$r_{NO} = k_{NO}C_{NO}\theta_{NH_3} \tag{6a}$$

$$r_{NO} = k_{NO}C_{NO}\theta^*_{NH_3}[1 - \exp(-\theta_{NH_3}/\theta^*_{NH_3})], \tag{6b}$$

where $k_{NO} = k^0_{NO}\exp(-E_{NO}/RT)$.

In the case of Eq. 6b, the rate of reaction is supposed to be essentially independent of the ammonia surface coverage above a critical NH_3 surface concentration ($\theta^*_{NH_3}$). This empirical rate expression is in line with the results of the NH_3 step-addition experiments reported in Figure 4A, which suggest that the rate of the SCR reaction is unaffected by changes in the ammonia surface concentration at high NH_3 coverage.

By adopting the same kinetic parameters for NH_3 adsorption–desorption estimated during the dynamic NH_3 adsorption study (and reported in Table 1), the fits shown in Figure 7 have been obtained for the ternary catalysts by global multiresponse nonlinear regression, minimizing the squared errors between the model predictions and the actual NH_3 and NO concentration profiles measured in the case of the NH_3 step feed experiments performed at 493 and 553. The results obtained both in the case of first-order kinetics in θ_{NH_3} (Eq.

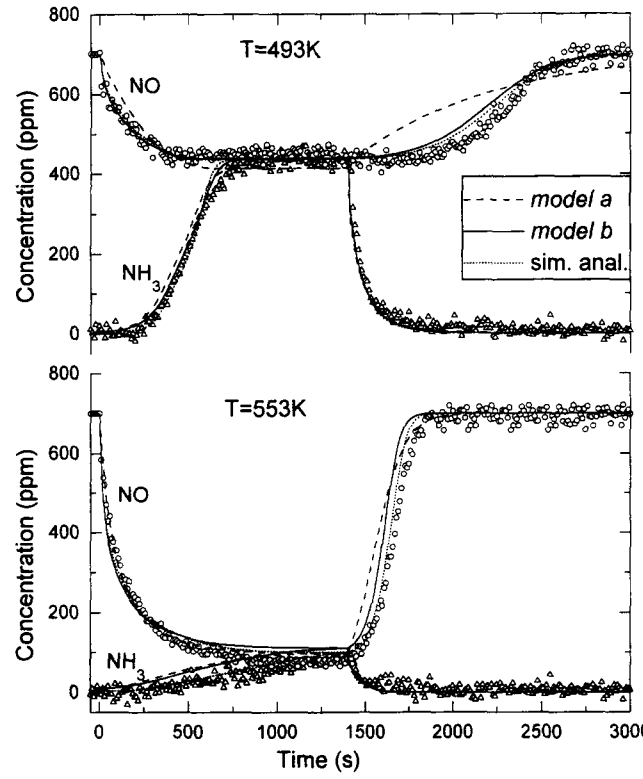

Figure 7. Step-feed and shutoff of NH_3 in $He+O_2$ (1% v/v) + NO (700 ppm) over the ternary WO_3–V_2O_5/TiO_2 catalyst: experimental data (symbols) and model fits.

Dashed lines: SCR kinetic *model a*; solid lines: SCR kinetic *model b* (Table 2); dotted lines: simultaneous analysis with the SCR kinetic *model b* (Table 3).

Table 2. Estimates of Kinetics Parameters for the SCR Reaction Over V_2O_5/TiO_2 and $V_2O_5-WO_3/TiO_2$ Catalysts*

Parameters	$V_2O_5-WO_3/TiO_2$	95% Confidence Limits	V_2O_5/TiO_2	95% Confidence Limits
k_a^0 (m^3/mol·s)	0.487	cost.	0.820	cost.
k_d^0 (1/s)	2.67×10^5	cost.	3.67×10^6	cost.
E_d^0 (kcal/mol)	22.9	cost.	25.8	cost.
α	0.405	cost.	0.310	cost.
Ω (mol/m^3)	270	cost.	209	cost.
k_{NO}^0 (m_3/mol s)	7.19×10^5	$\pm0.35\times10^5$	1.08×10^6	$\pm0.05\times10^6$
E_{NO} (kcal/mol)	14.2	±0.1	16.0	±0.1
$\theta^*_{NH_3}$	0.121	±0.012	0.076	±0.011

*Temkin-type NH_3 coverage dependence of the desorption energy and "modified" θ kinetics for the $DeNO_x$ reaction leading to the fits in Figures 6 and 7 (solid lines).

6a, dashed lines) and of "modified" θ kinetics (Eq. 6b, solid lines) are shown for two different temperatures. We note that only in the case of the "modified" θ kinetics (solid lines) is the model able to account adequately for the observed transient behaviors of all the species involved in the reaction, and in particular of NO at the lowest investigated temperature. Similarly, sastisfactory fits could be obtained in the case of the binary vanadia/titania catalyst only by adopting the "modified" θ kinetics but not using first-order kinetics. The values of the parameter estimates for both the binary and the ternary sample are reported in Table 2. An activation energy for the SCR reaction close to 15 kcal/mol has been estimated for both catalysts, in agreement with values in the literature (Wong and Nobe, 1984; Marshneva et al., 1995). It is worth emphasizing that the model satisfactorily accounts for the observed transient behaviors of the SCR reaction by simply superimposing the kinetics of the SCR reaction on the NH_3 adsorption–desorption kinetics, independently determined from the ammonia adsorption–desorption experiments performed in the absence of NO (Figures 2 and 3).

The soundness of the kinetics model is further confirmed by the analysis of the NO step-addition experiments, which could be nicely described on a purely predictive basis by using the kinetic parameter estimates reported in Table 2. As shown, for example, by the solid lines in Figure 6, in the case of the ternary $WO_3-V_2O_5/TiO_2$ sample, the model predicts successfully the results of the NO step-addition experiments performed at various temperatures; no parameter was adjusted to achieve the match between data and calculations shown in the figure. Similar results were obtained in the case of the binary V_2O_5/TiO_2 catalyst.

As an additional adequacy test, the mathematical model was eventually applied to analyze simultaneously the whole bulk of experimental data, including both the NH_3 adsorption–desorption runs and the unsteady SCR reaction runs. A Temkin-type adsorption coverage dependence of the desorption energy for ammonia and "modified" θ kinetics for the rate of nitrogen oxide reduction were used. The fit obtained for the ternary catalyst at two different temperatures (493 and 553 K) in the case of the simultaneous analysis is shown as dotted lines in Figure 7, and the corresponding parameter estimates are reported in Table 3. No significant differences are evident in the data fit with respect to *model b*, as is also indicated by the slight differences between the kinetic parameters estimated in the case of the simultaneous analysis (Table 3) and those previously obtained from the separate analysis of the NH_3 adsorption–desorption and surface reaction processes (Table 2). This confirms the adequacy of the adopted model for the description of the transient adsorption–desorption and reaction kinetics, as well as the virtual superposition of the two processes.

Discussion

Interaction of NH_3 and NO with the catalyst

The NH_3 adsorption–desorption experiments have pointed out that ammonia is strongly adsorbed on the catalyst surface and that surface heterogeneity must be considered when the NH_3 surface coverage is varied over a wide range. As shown by various characterization techniques, including FT-IR spectroscopy and TPD (Topsøe, 1991; Ramis et al., 1991; Lietti et al., 1993), surface heterogeneity is related to the presence of different adsorption sites for ammonia. These include both Lewis (associated with the Ti, W, and V components) and Bronsted (related to V and W) acid sites, which originate coordinated NH_3 and protonated NH_4^+ surface species, respectively. It has been reported that coordinated NH_3 species are thermally more stable than NH_4^+ surface species (Ramis et al., 1990; Lietti et al., 1993), and a debate is still open in the literature concerning the role of the coordinated and protonated ammonia in the SCR reaction (Ramis et al., 1990; Schneider et al., 1994; Topsøe et al., 1995a,b). In line with the well-documented surface heterogeneity, the results of our dynamic NH_3 adsorption–desorption experiments could not be reproduced by invoking a simple Langmuir approach, but were nicely fitted by a dynamic model that assumes a nonactivated NH_3 adsorption process and a Temkin-type coverage

Table 3. Estimates of the Kinetic Parameters for the SCR Reaction Over $V_2O_5-WO_3/TiO_2$ Catalysts*

Parameters	Simultaneous Analysis	95% Confidence Limits
k_a^0 (m^3/mol·s)	0.614	±0.026
k_d^0 (1/s)	1.99×10^5	$\pm0.05\times10^5$
E_d^0 (kcal/mol)	23.4	±0.2
α	0.448	±0.011
Ω (mol/m^3)	270	cost.
k_{NO}^0 (m^3/mol s)	8.39×10^5	$\pm0.026\times10^5$
E_{NO} (kcal/mol)	14.2	±0.08
$\theta^*_{NH_3}$	0.108	±0.01

*Temkin-type NH_3 coverage dependence of the desorption energy and "modified" θ kinetics for the $DeNO_x$ reaction leading to the fits reported in Figure 7 (simultaneous fit of NH_3 adsorption–desorption and SCR-$DeNO_x$ runs, dotted lines).

dependence of the desorption energy. Values of the activation energy for desorption in the range 18–26 kcal/mol (for $\theta_{NH_3} = 1$ and 0, respectively) have been estimated for the binary V_2O_5/TiO_2 sample. These results are in agreement with those reported by Srnak et al. (1992) who simulated a series of TPD experiments performed over TiO_2 and submonolayer vanadia/titania catalysts by invoking a nonactivated NH_3 adsorption process and suggesting the existence of three different adsorption sites with enthalpies of desorption ranging from 18 to 26 kcal/mol.

The NH_3 adsorption–desorption study has also been performed over the ternary V_2O_5–WO_3/TiO_2 catalyst, and similar results have been obtained with respect to the binary vanadia/titania sample. This eventually indicates that the acid characteristics of the two samples, with respect to the NH_3 adsorption–desorption, are quite similar.

In contrast to the strong NH_3 adsorption characteristics, NO does not appreciably adsorb on the catalyst surface. Nitrogen oxide adsorption has been observed over similar catalysts, but only in the case of reduced surfaces (Srnak et al., 1992). Accordingly, our results seem to rule out the possibility of a reaction between strongly adsorbed NH_3 and NO species, as also suggested by several authors (Srnak et al., 1992; Topsøe et al., 1995b). This conclusion is confirmed on a more general basis by the results of the dynamic study of the SCR reaction: indeed the transient behavior of the system upon stepwise changes of the NH_3 or NO reactor inlet concentration are typical of a reaction involving a strongly adsorbed species (NH_3) and a gas phase or weakly adsorbed species (NO). Therefore, our data are in line with the hypothesis of an Eley–Rideal mechanism for the SCR of NO by NH_3 (Topsøe et al., 1995b).

NH_3 adsorption sites vs. active sites

The dynamic study performed over both the binary and the ternary catalysts showed that the $DeNO_x$ reaction has a complex kinetic dependence on the ammonia surface coverage. Indeed it was found that the rate of the SCR reaction is a function of the ammonia surface concentration for NH_3 coverage below a characteristic "critical" value, whereas a much weaker dependence, if any, exists at high coverage. Indeed in this case the NO conversion was not affected for several minutes after the NH_3 shutoff. This suggests that a "reservoir" of adsorbed ammonia species available for the reaction is present on the catalyst surface. In this respect, the physicochemical characterization performed on the samples used in the present study and reported in detail elsewhere (Alemany et al., 1995; Lietti and Forzatti, 1994) indicates that V and Ti atoms are exposed at the surface in the case of the V_2O_5/TiO_2 catalyst, whereas V, Ti, and W are present in the case of the ternary sample. In both catalysts the V coverage is limited, and accordingly Ti and W atoms predominate on the surface, respectively. Temperature programmed desorption/reaction studies of NH_3 and of $NH_3 + NO$ (Srnak et al., 1992; Lietti and Forzatti, 1994; Lietti, 1996; Lietti et al., 1996) showed that ammonia is strongly held over Ti and over TiO_2-supported V- and W-species, but its reactivity in the SCR reaction varies considerably over the three oxides. Indeed the bare TiO_2 support is almost inert, whereas TiO_2-supported V- and W-oxides effectively convert NO, the reactivity of V being roughly one order of magnitude higher than that of W. Hence these results indicate that (1) Ti-, W-, and V-bonded ammonia surface species are present at the catalyst surface under reaction condition; (2) the presence of adsorbed NH_3, even at high temperature, is not a sufficient condition for the occurrence of the SCR reaction; (3) the NO consumption in the SCR reaction is principally ascribed to the presence of vanadium, which, however, represents only a minor fraction of the exposed catalyst surface ($< 20\%$); and (4) the adsorbed ammonia is almost entirely consumed in the SCR reaction: indeed no NH_3 was left on the catalyst surface after the SCR reaction had been completed, as indicated by TPD runs performed at the end of the transient experiments. On this basis, we speculate that the Ti- and W-bonded ammonia surface species, which are not readily consumed in the SCR reaction, act as an ammonia "reservoir" that are involved in the SCR reaction upon "migration" (possibly in the gas phase, by desorption and readsorption) to nearby reactive V sites. Accordingly the Ti- and W-bonded adsorbed ammonia species do not act simply as "spectators" in the SCR reaction, but can be involved as a "reservoir" in the NO consumption.

Kinetics of the $DeNO_x$ reaction

The dynamic behavior of the SCR reaction could be nicely fitted according to a one-dimensional heterogeneous unsteady PFR model that makes use of the NH_3 adsorption–desorption kinetics obtained independently and assumes a rate dependence of the SCR reaction on the ammonia surface concentration only at low NH_3 coverage. No good fit of the data could be achieved with a kinetic expression invoking a uniform dependence on the ammonia surface coverage over the whole experimental range of conditions. This suggests that the active catalyst sites responsible for ammonia activation represent only a fraction of the total adsorption sites for ammonia. As a matter of fact, in line with the hypothesis of V being the active element in the SCR reaction, the "critical" NH_3 coverage $\theta^*_{NH_3}$ is of the same order of magnitude of the catalyst V coverage ($\theta^*_{NH_3} = 0.12$ vs. $\theta_v = 0.12$ for the ternary catalyst and $\theta^*_{NH_3} = 0.08$ vs. $\theta_v = 0.21$ for the binary sample).

An obvious but important implication of the mechanistic considerations reported earlier is that approaches considering a single value for the NH_3 coverage (θ_{NH_3}) to represent the surface concentration of both adsorbed and reactive ammonia species are inadequate, in principle, to model the kinetics of the SCR reaction. A kinetic analysis based on the existence of an ammonia adsorption site and of an adjacent active site was proposed by Dumesic et al. (1993) and by Topsøe et al. (1995b). These authors carried out a steady-state microkinetic analysis of the SCR reaction and pointed out that the following reaction scheme is able to describe successfully the NO conversion and the ammonia slip data for vanadia/titania catalysts under stationary industrial SCR conditions.

$$NH_3 + M \Leftrightarrow NH_3\text{-}M$$

$$NH_3 - M + S \Leftrightarrow NH_3\text{-}S + M$$

$$NO + NH_3\text{-}S \Rightarrow N_2 + H_2O + S$$

where M represents an ammonia adsorption site and S is a reactive site. The M sites are associated with V^{5+}–OH sur-

face groups, whereas the S sites can be identified as $V^{5+}=O$ sites (Topsøe et al., 1995b). The SCR reaction is initiated by NH_3 adsorption on the $V^{5+}-OH$ Brønsted acid site; ammonia is then activated by the transfer of an H atom to the $V^{5+}=O$ site that is reduced to $V^{4+}-OH$. Gaseous or weakly adsorbed NO subsequently reacts with the activated NH_3 species, yielding the reaction products. The catalytic cycle is then completed with the oxidation of $V^{4+}-OH$ to $V^{5+}=O$.

It is noted, however, that no relevance is given in the proposed reaction scheme to the role of Ti sites, which do not participate directly in the SCR reaction, but on which ammonia is strongly adsorbed under the operating conditions typical of the SCR reaction (Topsøe, 1991; Ramis et al., 1990; Srnak et al., 1992; Lietti and Forzatti, 1994; Topsøe et al., 1995a). As previously discussed, it is likely that these Ti-bonded (and also W-bonded in the case of the ternary catalysts) ammonia species represent an ammonia "reservoir" that is involved in the SCR reaction by supplying the reactant NH_3 to the active sites, associated with the V component of the catalysts. It is noted that these effects are relevant only under transient conditions, where rapid changes in the NH_3 surface coverage occur, but could not be appreciated under steady-state conditions. This further indicates that dynamic conditions are best suited for the study of the complex interplay existing between the adsorbed and reactive NH_3 surface species, and accordingly to provide additional insight in to the mechanism of the SCR reaction. It is also noted that, according to our data, the distinction between the simple linear θ_{NH_3} kinetics and the more complex "modified" θ_{NH_3} kinetics vanishes at high temperatures, that is, at low ammonia surface coverage, as expected. Indeed in this case both the investigated kinetic models are adequate to describe the experimental data.

Activity of binary vs. ternary catalyst

The results of our kinetic analysis lead to a similar estimate of the activation energy of the SCR reaction for both the tested catalysts. The activity of the ternary sample in the SCR reaction is, however, much higher than that of the binary V_2O_5/TiO_2 catalyst with the same vanadia loading. The beneficial effect of WO_3 on the catalytic performances of $DeNO_x$ SCR vanadia-based catalysts has already been reported in the literature (Chen and Yang, 1992; Lietti et al., 1996). The present study does not provide direct evidence of the catalyst functions that are involved in the SCR reaction or of the role of the W component in the SCR reaction. However, the NH_3 dynamic adsorption–desorption study has shown that the acid characteristics of the two samples, as probed by the reactant NH_3, are quite similar. Accordingly, it is likely that factors other than the catalyst acidity should be primarily invoked to explain the remarkable increment of the catalyst activity that was observed upon WO_3 addition to the vanadia/titania sample. These aspects have already been investigated in detail elsewhere by means of different chemicophysical catalyst characterization techniques, including FT-IR, Raman-laser UV-Vis, EPR, and the temperature programmed desorption–reaction methods (Alemany et al., 1995; Lietti et al., 1996; Lietti, 1996; Paganini et al., 1996). In particular it has been shown that the significant increment of the rate of the $DeNO_x$ reaction that is observed by passing from the binary V_2O_5/TiO_2 to the ternary $V_2O_5-WO_3/TiO_2$ sample has been primarily ascribed to the enhanced redox properties of the catalyst due to tungsta addition. This indicates that the catalyst redox properties are among the key factors in controlling the reactivity of $V_2O_5-WO_3/TiO_2$ De–NO_x catalysts.

Table 4. Values of the Ratio r_d/r_{NO} Estimated at the Reactor Inlet and Outlet at Steady-State Conditions

	V_2O_5/TiO_2		$V_2O_5-WO_3/TiO_2$	
	553 K	623 K	493 K	553 K
Reactor inlet	9.2	2.0	4.3	0.7
Reactor outlet	10.7	3.0	4.9	1.7

Relative rates of the steps in the kinetic scheme

The analysis of the parameter estimates obtained over both the binary and the ternary samples also leads to additional significant implications concerning the steady-state kinetics of the SCR reaction. Considering that, at steady-state conditions,

$$r_a = r_d + r_{NO},$$

it follows that, if r_{NO} is negligible with respect to r_d ($r_{NO} \ll r_d$),

$$r_a \approx r_d$$

and NH_3 adsorption equilibrium can be assumed. Table 4 presents values of the r_d/r_{NO} ratio (i.e., the ratio of the rate of ammonia desorption to the rate of ammonia consumption by the SCR reaction) estimated at the reactor inlet and outlet at various temperatures over both the binary and the ternary catalyst for steady-state conditions. The values do not change significantly between the inlet and the outlet of the reactor, and decrease upon increasing the temperature. The r_d/r_{NO} ratio is greater than 1 at 553 K and in the case of the less active vanadia/titania catalyst, but it is close to 1 at high temperature and over the most active vanadia–tungsta/titania catalyst.

Thus, the data in Table 4 point out that the assumption of equilibrated ammonia adsorption, which was used by several authors in the derivation of steady-state kinetic expressions for the SCR reaction (Beekman and Hegedus, 1991; Tronconia and Forzatti, 1992; Dumesic et al., 1993), is not always applicable under steady-state $DeNO_x$ conditions. Particularly, it is incorrect at high temperatures and over active catalysts, where no single rate-controlling step can be identified. Work is in progress in order to arrive at a steady-state kinetic expression for the SCR reaction that takes into account all the mechanistic and kinetic features observed in the present study.

Conclusions

The transient-response method has provided a powerful tool for the study of the dynamics of the adsorption–desorption of NH_3 and of the $DeNO_x$–SCR reaction over

V_2O_5/TiO_2 model-based catalysts. The major results can be summarized as follows:

1. NH_3 is strongly and similarly adsorbed on both V_2O_5/TiO_2 and $V_2O_5-WO_3/TiO_2$ catalyst samples. Surface heterogeneity must be considered to describe the kinetics of NH_3 adsorption–desorption when the surface coverage is varied over a wide range. In this case a model assuming a nonactivated NH_3 adsorption process and a Temkin-type coverage dependence of the desorption enregy is well suited to represent the dynamic data, with values of the activation energy for desorption at zero-coverage ranging from 22 to 26 kcal/mol.

2. In contrast to NH_3, NO does not adsorb appreciably on the catalyst surface. Consequently, the possibility of a reaction between coadsorbed NH_3 and NO according to a Langmuir–Hinshelwood mechanism is ruled out. On the other hand, the transient behavior of the SCR reaction upon stepwise changes of the NH_3 or NO feed concentrations is in line with an Eley–Rideal pathway involving a strongly adsorbed species (NH_3) and a gaseous or weakly adsorbed species (NO).

3. Over both the binary and the ternary catalyst the rate of the $DeNO_x$ reaction is virtually independent of the ammonia surface concentration for NH_3 coverage above a characteristic "critical" value. This is explained by assuming that a "reservoir" of adsorbed ammonia species, possibly adsorbed onto poorly active (but most abundant) W and Ti sites, are present on the catalyst surface and are available for the reaction once the NH_3 gas-phase concentration is decreased. According to this picture the Ti- and W-bonded adsorbed ammonia species do not act simply as "spectators" in the SCR reaction, but are dynamically involved in the consumption of NO, which occurs on active V sites.

4. The observed dynamic behavior of the SCR reaction could be nicely fitted according to a one-dimensional hetergoeneous unsteady PFR model, superimposing the NH_3 adsorption–desorption process, with kinetics obtained by the independent ammonia adsorption study, to the SCR reaction. The most adequate rate expression for the $DeNO_x$ reaction is independent of the ammonia surface coverage at high θ_{NH_3}, and becomes first order in respect to the ammonia surface concentration only below a "critical" NH_3 coverage ($\theta^*_{NH_3}$). Values of $\theta^*_{NH_3}$ close to 0.1 have been estimated for both the binary and the ternary catalysts: these values are of the same order of magnitude as the V coverage of the samples.

5. The binary and the ternary catalyst samples exhibit similar acid properties but different activities in the SCR reaction: this was previously associated with the superior redox properties of the WO_3-containing catalyst.

6. The analysis of the rate-parameter estimates obtained over both the binary and the ternary samples indicates that the assumption of equilibrated ammonia adsorption may be incorrect under steady-state $DeNO_x$ conditions, specifically at high temperature and overactive catalysts.

Acknowledgments

This work performed under contract with ENEL/DSR/CRT Pisa. The financial support of Ministero dell'Università e della Ricerca Scientifica e Tecnologica (MURST) is also acknowledged.

Notation

A = parameter for the surface coverage dependence
B = parameter for the surface coverage dependence, cal/mol
C_{NH_3} = gas-phase NH_3 concentration, mol/m^3
C_{NO} = gas-phase NO concentration, mol/m^3
E_a = activation energy for NH_3 adsorption, kcal/mol
E_{NO} = activation energy for the $DeNO_x$ reaction, kcal/mol
k^0_a = preexponential factor for NH_3 adsorption rate constant, $m^3 \cdot mol^{-1} \cdot s^{-1}$
k^0_d = preexponential factor for NH_3 desorption rate constant, s^{-1}
k^0_{NO} = preexponential factor for the $DeNO_x$ reaction rate constant, $m^3 \cdot mol^{-1} \cdot s^{-1}$
k_{NO} = kinetic constant for the $DeNO_x$ reaction rate constant, $m^3 \cdot mol^{-1} \cdot s^{-1}$
R = ideal gas constant, cal/(mol·K)
r_a = rate of adsorption, s^{-1}
r_d = rate of desorption, s^{-1}
r_{NO} = rate of NO consumption, s^{-1}
v = interstitial gas velocity, m/s
z = reactor axial coordinate, m
α = parameter for the surface coverage dependence
ϵ = void fraction of the catalyst bed
θ_{NH_3} = NH_3 surface coverage
$\theta^*_{NH_3}$ = critical NH_3 surface coverge
σ = parameter for the surface coverage dependence
$\Omega = [(1-\epsilon)/\epsilon] \cdot \Omega'$
Ω' = catalyst NH_3 adsorption capacity, mol_{NH_3}/m^3

Subscripts

a = adsorption
d = desorption

Literature Cited

Alemany, L., L. Lietti, N. Ferlazzo, P. Forzatti, G. Busca, E. Giamello, and F. Bregani, "Reactivity and Physicochemical Characterization of V_2O_5-WO_3/TiO_2 De-NO_x Catalysts," *J. Catal.*, **155**, 117 (1995).

Andersson, S. L., P. L. T. Gabrielsson, and C. U. I. Odenbrand, "Reducing NO_x in diesel exhausts by SCR technique: Experiments and Simulations," *AIChE J.*, **40**(11), 1911 (1994).

Beekman, J., and L. Hegedus, "Design of Monolith Catalysts for Power Plant NO_x Emission Control," *Ing. Eng. Chem. Res.*, **30**, 969 (1991).

Bond, G. C., and S. F. Tahir, "Vanadium Oxide Monolayer Catalysts. Preparation, Characterization and Catalytic Activity," *Appl. Catal.*, **71**, 1 (1991).

Bosch, H., and F. Janssen, "Catalytic Reduction of Nitrogen Oxides. A Review on the Fundamentals and Technology," *Catal. Today*, **2**, 369 (1988).

Chen, J. P., and R. T. Yang, "Role of WO_3 in Mixed V_2O_5 – WO_3/TiO_2 Catalysts for Selective Catalytic Reduction of Nitric Oxide with Ammonia," *Appl. Catal. A: Gen.*, **80**, 135 (1992).

Dumesic, J. A., N.-Y. Topsøe, T. Slabiak, P. Morsing, B. S. Clausen, E. Tornqvist, and H. Topsøe, "Microkinetic Analysis of the Selective Catalytic Reduction (SCR) of Nitric Oxide Over Vanadia/Titania-based Catalysts," *New Frontiers in Catalysis*, L. Guczi et al., eds., Elsevier Science, Amsterdam, Netherlands (1993).

Finlayson, B., *Non Linear Analysis in Chemical Engineering*, McGraw-Hill, New York (1980).

Forzatti, P., and L. Lietti, "Recent Advances in De-NO_xing Catalysis for Stationary Applications," *Heter. Chem. Rev.*, **3**(1), 33 (1996).

Froment, G., and K. Bischoff, *Chemical Reactor Analysis and Design*, Wiley, New York (1979).

Hindmarsh, A. C., "Odepack: A Systematized Collection of Ode Solvers," *Scientific Computing*, R. S. Stepleman et al., eds., North-Holland, Amsterdam (1983).

Kobayashi, H., and M. Kobayashi, "Transient Response Method in Heterogeneous Catalysis," *Catal. Rev.-Sci. Eng.*, **10**, 139 (1974).

Lietti, L., P. Forzatti, G. Ramis, G. Busca, and F. Bregani, "Potassium Doping of Vanadia/Titania de-NOxing Catalysts: Surface Characterization and Reactivity Study," *Appl. Catal. B: Environ.*, **3**, 13 (1993).

Lietti, L., "Reactivity of V_2O_5-WO_3/TiO_2 de-NO_x Catalysts by Transient Methods," *Appl. Catal. B: Environ.*, **10**, 281 (1996).

Lietti, L., and P. Forzatti, "Temperature Programmed Desorption/Reaction of Ammonia Over V_2O_5/TiO_2 De-NO_xing Catalysts," *J. Catal.*, **147**, 241 (1994).

Lietti, L., P. Forzatti, and F. Bregani, "Steady-State and Transient Reactivity Study of TiO_2-supported V_2O_5-WO_3 De-NO_x Catalysts: Relevance of the Vanadium-Tungsten Interaction on the Catalytic Activity," *Ind. Eng. Chem. Res.*, **35**(11), 3884 (1996).

Marshneva, V. I., E. M. Slavinskaya, O. V. Kalinkina, G. V. Odegova, E. M. Moroz, G. V. Lavrova, and A. N. Salanov, "The Influence of Support on the Activity of Monolayer Vanadia-Titania Catalysts for Selective Catalytic Reduction of NO with Ammonia," *J. Catal.*, **155**, 171 (1995).

Mears, D. E., "Tests for Transport Limitations in Experimental Catalytic Reactors," *Ind. Eng. Chem. Process Des. Dev.*, **10**(4), 541 (1971).

Noskov, A., L. Bobrova, G. Bunimovich, O. Goldman, A. Zagoruiko, and Y. Matros, "Application of the Non-stationary State of a Catalyst Surface for Gas Purification from Toxic Impurities," *Catal. Today*, **27**, 315 (1996).

Odenbrand, C. U. I., A. Bahamonde, P. Avila, and P. Blanco, "Kinetic Study of the Selective Reduction of Nitric Oxide Over Vanadia-Tungsta-Titania/Sepiolite Catalyst," *Appl. Catal. B: Environ.*, **5**, 117 (1994).

Orsenigo, C., A. Beretta, P. Forzatti, J. Svachula, E. Tronconi, F. Bregani, and A. Baldacci, "Theoretical and Experimental Study of the Interaction Between NO_x Reduction and SO_2 Oxidation over DeNO_x-SCR Catalysts," *Catal. Today*, **27**, 15 (1996).

Paganini, M. C., L. Dall'Acqua, E. Giamello, L. Lietti, P. Forzatti, and G. Busca, "An EPR Study of the Surface Chemistry of the Vanadia-Tungsta-Titania Catalyst: State of V(IV) and Redox Behavior," *J. Catal.*, **166**, 195 (1997).

Ramis, G., G. Busca, F. Bregani, and P. Forzatti, "Fourier Transform-Infrared Study of the Adsorption and Coadsorption of Nitric Oxide, Nitrogen Dioxide and Ammonia on Vanadia-Titania and Mechanism of Selective Catalytic Reduction," *Appl. Catal.*, **64**, 259 (1990).

Ramis, G., G. Busca, F. Bregani, and P. Forzatti, "An FT-IR Study of the Reaction of NO with Adsorbed Ammonia on the Surface of Vanadia-Titania DeNO_xing Catalysts," *Catal. Sci. Tech.*, **1**, 189 (1991).

Ramis, G., G. Busca, P. Forzatti, C. Cristiani, L. Lietti, and F. Bregani, "Characterization of Tungsta-Titania Catalysts," *Langmuir*, **8**, 1744 (1992).

Schneider, H., S. Tschudin, M. Schneider, A. Wokaun, and A. Baiker, "*In Situ* Diffuse Reflectance FTIR Study of the Selective Catalytic Reduction of NO by NH_3 over Vanadia-Titania Aerogels," *J. Catal.*, **147**, 5 (1994).

Srnak, T. Z., J. A. Dumesic, B. S. Clausen, E. Törnqvist, and N. Y. Topsøe, "Temperature-programmed Desorption/Reaction and *In Situ* Spectroscopic Studies of Vanadia/Titania for Catalytic Reduction of Nitric Oxide," *J. Catal.*, **135**, 246 (1992).

Topsøe, N.-Y., "Characterization of the Nature of Surface Sites on Vanadia-Titania Catalysts by FTIR," *J. Catal.*, **128**, 499 (1991).

Topsøe, N-Y., H. Topsøe, and J. A. Dumesic, "Vanadia/Titania Catalysts for Selective Catalytic Reduction (SCR) of Nitrogen Oxide by Ammonia: I. Combined Temperature Programmed *in situ* FTIR and On-line Mass Spectroscopy Studies," *J. Catal.*, **151**, 226 (1995a).

Topsøe, N.-Y., H. Topsøe, and J. A. Dumesic "Vanadia/Titania Catalysts for Selective Catalytic Reduction (SCR) of Nitrogen Oxide by Ammonia: II. Studies of Active Sites and Formulation of Catalytic Cycles," *J. Catal.*, **151**, 241 (1995b).

Tronconi, E., and P. Forzatti, "Modeling and Experimental Verification of TPD from Porous Catalysts," *Chem. Eng. Sci.*, **41**, 2541 (1986).

Tronconi, E., and P. Forzatti, "Adequacy of Lumped Parameter Models for SCR Reactors with Monolith Structure," *AIChE J.*, **38**, 201 (1992).

Tronconi, E., L. Lietti, P. Forzatti, and S. Malloggi, "Experimental and Theoretical Investigation of the Dynamics of the SCR-DeNOx Reaction," *Chem. Eng. Sci.*, **51**(11), 2965 (1996).

Tufano, V., and M. Turco, "Kinetic Modeling of Nitric Oxide Reduction Over a High-Surface Area V_2O_5/TiO_2 Catalysts," *Appl. Catal. B: Environ.*, **2**, 9 (1993).

Vermaire, D. C., and P. C. van Berge, "The Preparation of WO_3/TiO_2 and WO_3/Al_2O_3 and Characterization by Temperature-programmed Reduction," *J. Catal.*, **116**, 309 (1989).

Wong, W. C., and K. Nobe, "Kinetics of NO Reduction with NH_3 on "Chemical Mixed" and Impregnated V_2O_5/TiO_2 Catalysts," *Ind Eng. Chem. Prod. Res. Dev.*, **23**, 564 (1984).

Manuscript received Jan. 27, 1997, and revision received June 2, 1997.